Phonon-wind-based transport in InGaAs-InP quantum well under intense optical excitation

A. F. G. Monte, S. W. da Silva, J. M. R. Cruz, P. C. Morais, and A. S. Chaves
Universidade de Brasília, Instituto de Física, Núcleo de Física Aplicada, Caixa Postal 04455, 70919-970, Brasília, Distrito Federal, Brazil
(Received 21 December 1999)

The microluminescence surface scan technique (MSST) is used to investigate the lateral transport of photocarriers in a thin InGaAs-InP quantum well, under high optical excitation intensity (0.3 to 30 KW/cm^2) and in the temperature range from 7 to 200 K. The size of the in-plane photocarrier distribution depends on both optical excitation intensity and temperature. A phonon-wind-driven mechanism is used to explain the behavior of the distribution at temperatures below 15 K. Further, the attenuation of the phonon flux during the photocarrier cloud expansion plays a key role in the phonon-wind mechanism. Finally, it is found that the phonon wind becomes quenched at high optical excitation intensity, which is probably correlated to an increasing carrier velocity greater than the sound velocity.

I. INTRODUCTION

Investigation of the transport of photoexcited carriers in bulk[1,2] and thin layer semiconductor materials[3–8] has attracted a lot of interest due to both fundamental and technological reasons. Experimental techniques which incorporate spatial as well as time-resolved capabilities have been used to study the underlying mechanisms governing the two-dimensional (2D) transport of photocarriers. Though experiments involving the effect of the temperature, layer thickness, optical excitation intensity and photon energy have been carried out, several aspects related to the 2D-transport properties of photocarriers remain unclear. Special attention has been devoted to the investigation of the diffusion of photocarriers under low[4–6] and high[7,8] optical excitation regimes, where quite different behaviors have been observed. Carrier diffusion in GaAs-AlGaAs quantum wells (QW's) has been investigated through time-of-flight (TOF) measurements[3–5] and pump-probe techniques,[6,7] as a function of temperature, layer thickness, optical excitation intensity and photon energy. In the microluminescence surface scan technique (MSST) used in this work,[9] a tightly focused laser beam (few microns wide) is used to excite the sample surface, and the lateral spread of electrons and holes is observed by scanning the microluminescence image at the system's focal plane.[10] In this work, the lateral size of the photoexcited carrier cloud is investigated under different conditions, from which important information concerning the 2D-transport mechanism is obtained. An undoped InGaAs-InP single QW was used to perform the experiments at different optical excitation intensities (I) and temperatures (T). In particular, we focus our attention in the high optical excitation and low temperature conditions. Under such conditions, our data are consistent with a phonon-wind driving the 2D distribution of photocarriers.[4,5,7,8] The attenuation of the phonon flux during the photocarrier cloud expansion is included into the phonon-wind mechanism, thus accounting for the relationship between theory and experiment.

II. EXPERIMENT

The lattice-matched InGaAs-InP single QW used in this work was grown by Vapor Levitation Epitaxy.[11] The nominally undoped sample consists of a 0.6 μm-thick InP buffer layer epitaxially grown on top of an InP substrate, followed by a 110 Å wide InGaAs QW and terminated with a 600 Å thick InP cap layer. The sample was mounted in a temperature-controlled optical cryostat and optically excited using a CW Ar^+-ion laser tuned at 514 nm, which provides energy excitation above the InP band gap. The laser beam is focused down to a 5 μm-diameter spot, and the lateral photoluminescence (PL) measurements had a resolution of about 2 μm. The radial PL intensity distribution is chopped, synchronously amplified and measured using a nitrogen-cooled Germanium detector, as described elsewhere.[10] At the first moment, nonresonant photoexcitation creates highly energetic free electrons and free holes all across the structure, which are quickly captured by the InGaAs single QW. Thermalization with the lattice is achieved mostly through emission of longitudinal optical and acoustic phonons, the excess carrier density and gradient give rise to spontaneous radiative recombination and lateral carrier diffusion. Spontaneous recombination is the main source of the PL signal. As the photogenerated carrier density is assumed to be much higher than any residual dopant density, we have assumed the photoinduced hole density (p) to match the photoinduced electron density (n).

III. RESULTS AND DISCUSSIONS

The optical excitation intensity was set at a level strong enough to produce areal carrier densities in the range of 10^{11} to 10^{13} cm^{-2}, where recombination is predominantly radiative. In a semiconductor QW, the carrier system will be excitonic at low carrier density and electron-hole plasma like at high carrier density. This will result in a change of the carrier type within the spatial carrier distribution; at the center, the carrier system will be an electron-hole plasma, and in the wings, there will be predominantly excitons. The two species have different transport properties, what makes the spatially resolved luminescence spectra useful, since it can distinguish between an excitonic and an electron-hole plasma like system. Due to signal decrease we were not able to obtain spectra at the tail of the distribution, where it should be excitonic

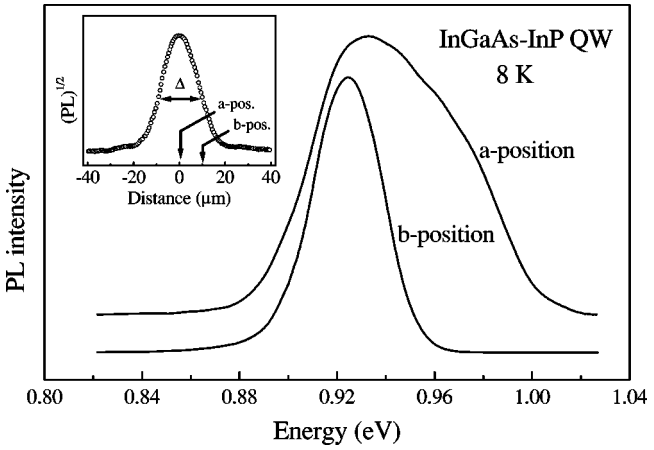

FIG. 1. PL spectra taken at different positions on the spatial carrier distribution. The spatial profile of the carrier distribution with width Δ is shown in the inset. Spectrum *a* is taken at the center of the carrier distribution while spectrum *b* is taken at about the half width.

like. We have observed in Fig. 1 that the luminescence spectra are not excitonic up to the half width of the distribution. As a result, the transport properties do not change appreciably in the same spatial range.

A typical spatial profile of the carrier distribution, which is obtained from the square root of the spectrally integrated PL intensity, is shown in the inset of Fig. 1. The quantity Δ is the full width at half maximum (FWHM) of the carrier distribution. The photocarriers are mainly confined in the InGaAs layer, so that the carrier transport can be described by a two-dimensional diffusion equation. In the steady-state regime, the diffusion equation describing the ambipolar plasma in polar coordinates reads[10]

$$D\frac{1}{r}\frac{\partial}{\partial r}\left[r\frac{\partial n}{\partial r}\right]=G(r)-\frac{n}{\tau}-Bn^2, \tag{1}$$

where D is the effective diffusion coefficient, τ is the effective carrier lifetime, and B is the radiative recombination coefficient. $G(r)$ is the photocarrier generation term provided by a Gaussian-shaped laser spot. As long as both the linear and quadratic terms are kept in the right-hand side of Eq. (1), numerical simulation shows that a Gaussian function represents a reasonable solution for $n(r)$. The carrier diffusion length ($L=\sqrt{D\tau}$) is then obtained from the best simulated curve going through the experimental points (see inset of Fig. 1), and is proportional to the FWHM of the carrier distribution ($L\propto\Delta$).

As shown in Fig. 2, below about 15 K, the diffusion length increases for decreasing temperatures. Only a very pronounced increase in the diffusivity at decreasing temperatures could account for that change in the behavior of $L(T)$. The temperature dependence of the FWHM (Δ) of the carrier distribution, at an optical excitation intensity on the order of 30 KW/cm^2, is shown in the inset of Fig. 2. In the temperature range of 50 to 200 K, Δ goes linearly with the temperature. The increase of the diffusion length with temperature means that the particle diffusivity is not limited by phonon scattering; in fact, if the thermal phonons represent the main scattering mechanism, the diffusivity would decrease with increasing temperature. On the other hand, if static impurities represent the only particle scattering mechanism, the diffusivity D should be proportional to the particle thermal velocity, and therefore $D\propto T^{1/2}$.[6] Considering that the radiative lifetime of the particles is $\tau\propto T^{3/2}$,[12] one concludes that $L=\sqrt{D\tau}\propto T$. On these grounds, we conclude that in the temperature range 50 K $<T<$ 200 K the carrier plasma presents a diffusive behavior were static impurities are the dominant scattering centers. Further, the assumption of a phonon-wind is introduced in the low temperature range ($T<15$ K), once this mechanism pushes the carriers away from the optical excitation region, thus spreading up the plasma expansion. The reduction in Δ up to 15 K, when T increases (see Fig. 2), is consistent with the picture of a sharp decrease of the diffusion coefficient as a result of the thermal damping of the phonon-wind-driven force. Specifically, the phonon-wind driven force should be greatly reduced when the bath temperature is raised to the point where the phonon mean-free-path becomes comparable to the width of the carrier distribution. Such a behavior has been previously observed in GaAs-AlGaAs QW's, under high optical excitation intensity (carrier density around 10^{11} cm^{-2}),[7] and low optical excitation intensity (carrier density below 10^{11} cm^{-2}).[4–6]

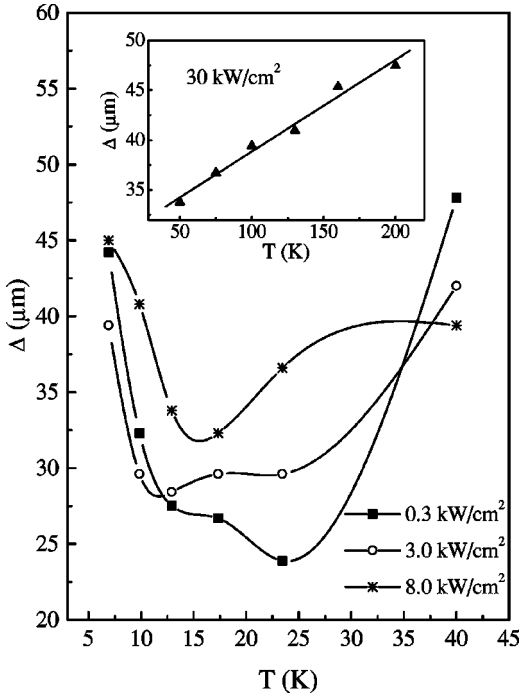

FIG. 2. Spatial carrier distribution (Δ) as a function of the temperature, at different optical excitation intensities. Lines are only guides to the eyes. The abrupt increase of Δ below 15 K was associated with the increase of the diffusivity due to the phonon-wind mechanism. The temperature dependence of Δ under high optical excitation intensity is shown in the inset.

In order to investigate the 2D-carrier expansion mechanism in the two different regimes, we analyzed in Fig. 3 the width of the carrier distribution (Δ) as a function of the optical excitation intensity (I) at different temperatures. We first observe that the excitation intensity dependence of Δ, at 13 K, is qualitatively consistent with the in-plane expansion of the photocreated carriers outside the laser spot region by a phonon-wind-driven mechanism.[7] In the phonon-wind

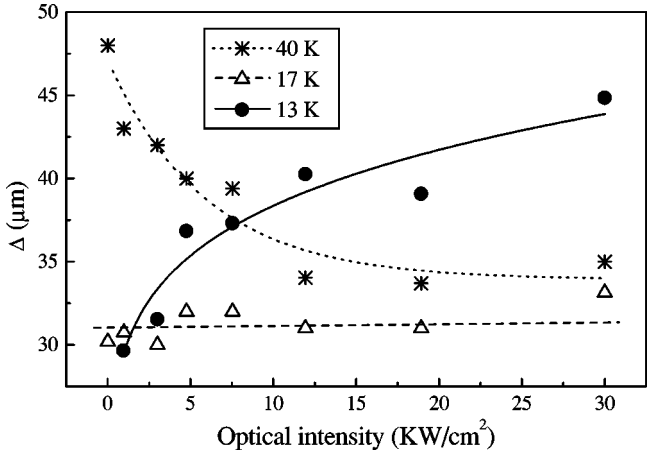

FIG. 3. Spatial carrier distribution (Δ) as a function of the optical excitation intensity. The excitation behavior changes drastically as the temperature is increased. At 13 K, the behavior of the carrier profile is dominated by the phonon wind mechanism. At 40 K, since the phonon wind is not effective, the behavior is dictated by the carrier lifetime. At 17 K, the dominant characteristic of the curve is a crossover between the two behaviors (13 K and 40 K).

mechanism, the thermalization of localized high-density photocarriers works as an important source of non-equilibrium acoustic phonons, which in turn propagate outward from the optically excited spot. This collective phonon motion interacts with the carriers by transferring momentum. In the simplest phonon-wind-driven picture the photoexcited carriers are submitted to a wind force given by $F=\gamma P(1-\nu/\nu_s)$, where γ is a coupling constant, P is the phonon flux, ν is the carrier drift velocity and ν_s the sound velocity. The drift velocity is also related to the wind force through $\nu=\mu F/q$, where q and μ are the carrier charge and carrier mobility, respectively. The two expressions above can be coupled together to yield $\nu\simeq\mu\gamma P/q$, in the limit of $\nu\ll\nu_s$. Within the usual conservative approach, with no phonon attenuation, the phonon flux is given by $P=(\rho_0/\rho)P_0$, where ρ_0 and ρ represent different radial positions in the InGaAs layer plane with respect to the center of the laser spot, and P_0 depends only on the optical excitation intensity. By combining the last two expressions together one obtains $\nu\simeq(\mu\gamma/q)(\rho_0/\rho)P_0$. At this point, we argue that the observed Δ represents the characteristic length covered during the characteristic lifetime (τ_0). The average carrier velocity would be reasonably described by $\nu\simeq\Delta/2\tau_0$ and, consequently, Δ would be given by

$$\Delta^2\simeq aP_0, \tag{2}$$

where $a=4\mu\gamma\rho_0\tau_0/q$. The conservative model for the total number of phonons leading to Eq. (2) explains the increase of Δ with increasing excitation intensity. However, better results are obtained if a nonconservative model is assumed. To describe the phonon flux attenuation, the following expression is introduced: $P=P_0(\rho_0/\rho)\exp(-b\rho)$, where b is a characteristic parameter to be obtained from the fit of the experimental data. Following the same arguments used above to derive Eq. (2), Δ is now described through

$$\Delta^2\exp\left(\frac{b\Delta}{2}\right)\simeq aP_0. \tag{3}$$

The solid line in Fig. 3 represents the best fit of the experimental data assuming attenuation of the phonon flux. The attenuation of the phonon flux have been accounted for by the absorption of phonons by cool carriers.[8]

The optical intensity dependence of the plasma expansion at 40 K (see Fig. 3), can be understood in terms of the carrier lifetime. The carrier density dependence of the carrier lifetime is known to vary by several orders of magnitude, from 0.1 μs at 10^{14} cm^{-3} to 10 ps at 10^{19} cm^{-3}.[13] Therefore, as the optical excitation intensity increases, thus increasing n, the diffusion length is expected to decrease due to the reduction of the carrier lifetime. Similar behavior was also confirmed at higher temperatures.[14] In contrast to what happens at 13 K, where the spatial distribution obeys the excitation dependence of Eq. (3), at 17 K, even for high optical excitation intensities, the spatial carrier distribution does not change. The data shown at 17 K support the existence of the two distinct carrier diffusion mechanisms and represent the crossover condition between them. The carrier lifetime has another implication on the phonon-wind force since it changes the particle velocity. The phonon-wind driven force should reduce if the particle velocity is greater than the sound velocity ($\nu_s=5\times10^5$ cm/s). This effect may really take place at high optical excitation (see inset of Fig. 2), where we have observed a less pronounced effect on the plasma expansion at 30 KW/cm^2. For this optical power density, we can estimate a carrier density on the order of 1×10^{13} cm^{-2}, which represents a carrier lifetime of 100 ps.[13] Thus, if we take the width of the plasma expansion (Δ) on the order of 35 μm at 30 KW/cm^2, and using the simple relation $\nu=\Delta/2\tau$, the particle velocity should be on the order of 18×10^6 cm/s, which is much greater than the sound velocity. Therefore, the phonon-wind driven force should be highly reduced at this optical power density.

IV. CONCLUSIONS

In summary, we infer that ionized impurity scattering and radiative recombination determine the carrier expansion process at higher temperatures. However, we found that the phonon-wind-driven mechanism plays a key role in the explanation of the carrier expansion on the low temperature range (below 15 K). The hypothesis of the phonon flux attenuation, in contrast to the conservative picture, leads to a better agreement between the data and the phonon-wind-driven theory.

ACKNOWLEDGMENTS

We are grateful to Dr. H. M. Cox for providing the sample used in this work and also the financial support from TWAS and the Brazilian agencies FAP-DF and CNPq.

[1] J. Doehler and J.M. Worlock, Phys. Rev. Lett. **41**, 980 (1978).
[2] M.R. Junnarkar and R.R. Alfano, Phys. Rev. B **34**, 7045 (1986).
[3] H. Hillmer, A. Forchel, S. Hansmann, M. Morohashi, E. Lopez, H.P. Meier, and K. Ploog, Phys. Rev. B **39**, 10 901 (1989).
[4] H. Hillmer, A. Forchel, and C.W. Tu, Phys. Rev. B **45**, 1240 (1992).
[5] Y. Takahashi, K. Muraki, S. Fukatsu, S.S. Kano, Y. Shiraki, and R. Ito, Solid State Commun. **88**, 677 (1993).
[6] H.W. Yoon, D.R. Wake, J.P. Wolfe, and H. Morkoç, Phys. Rev. B **46**, 13 461 (1992).
[7] L.M. Smith, J.S. Preston, J.P. Wolfe, D.R. Wake, J. Klem, T. Henderson, and H. Morkoç, Phys. Rev. B **39**, 1862 (1989).
[8] A.E. Bulatov and S.G. Tikhodeev, Phys. Rev. B **46**, 15 058 (1992).
[9] A.F.G. Monte, J.M.R. Cruz, and P.C. Morais, Rev. Sci. Instrum. **68**, 3890 (1997).
[10] A.F.G. Monte, J.M.R. Cruz, P.C. Morais, and H.M. Cox, Solid State Commun. **109**, 163 (1998); A.F.G. Monte, S.W. da Silva, J.M.R. Cruz, P.C. Morais, and H.M. Cox, J. Appl. Phys. **85**, 2866 (1999).
[11] H.M. Cox, S.G. Hummel, and V.G. Keramidas, J. Cryst. Growth **79**, 900 (1986).
[12] R.N. Hall, Proc. IEEE **106**, 923 (1959); M. Gallant and A. Zamel, Appl. Phys. Lett. **52**, 1686 (1988).
[13] R.K. Ahrenkiel, R. Ellingson, S. Johnston, and M. Wanlass, Appl. Phys. Lett. **72**, 3470 (1998).
[14] A.F.G. Monte, S.W. da Silva, J.M.R. Cruz, P.C. Morais, and H.M. Cox, Physica B **273**, 963 (1999).